Characterization of Post-Mining Soil and Solid Waste from Silica Sand Purification

Bernadetha Susianti[1,2], Idaa Warmadewanthi[1*], Bieby Voijant Tangahu[1]

[1] Department of Environmental Engineering, Faculty of Civil, Planning, and Geo-Engineering, Sepuluh Nopember Institute of Technology, ITS Sukolilo Campus, Surabaya 60111, East Java – Indonesia
[2] PT. Jara Silica, Village Jenu, Tuban Regency 62352, East Java – Indonesia
* Corresponding author's e-mail: warma@its.ac.id

ABSTRACT

Post-mining soil and solid waste from the silica sand refining industry is widespread and the potential long-term impact of toxic metals and metalloids is a significant and under-appreciated issue. This study presents the characteristics of post-mining soil and solid waste resulting from silica sand purification to observe its physical, chemical, and biological composition. Analysis of the physical properties was carried out with reference to ASTM 112-10 and the results show that post-mining soil contains 36.95% sand, 18.80% clay, and 42.74% silt, with coefficients of permeability and porosity of 0.69×10^{-6} cm·s^{-1} and 35.84%, respectively. Meanwhile, the solid waste contains 43.35% sand, 35.96% clay, and 20.68% silt with coefficients of permeability and porosity of 1.49×10^{-6} cm·s^{-1} and 51.12%. The overall mineralogy and morphology of both samples showed that they have the same chemical composition as gehlenite ($Ca_2Al_2SiO_7$), spinel ($MgAl_2O_4$), akermanite ($Ca_2MgSi_2O_7$), monticellite ($CaMgSiO_4$), aluminum oxide (Al_2O_3), magnetite (Fe_3O_4), and hematite (Fe_2O_3) supports this data. The chemical composition of both samples is SiO_2, Al_2O_3, CaO, and MgO, but the post-mining soil has lower heavy metal and nutrient contents compared to solid waste. Meanwhile, solid waste has a high content of heavy metals and nutrients due to washing and bonding from the silica sand purification process. The abundance of bacteria (Colony Forming Unit) for the 10^{-4} and 10^{-5} dilutions in post-mining soil was 1.59×10^3 and not detected, while in the solid waste, 4.10×10^5 and 1.64×10^5 were found, respectively. This study can be used as base values for modifying the two samples, which can be applied in mining land reclamation.

Keywords: characteristic, post-mining, purification, soil, solid waste.

INTRODUCTION

Nowadays, silica sand is the most widely used raw material for several high technology applications (Santos et al., 2015; Ashrafi-Shahri et al., 2019). It is a unique material for crystalline silicon manufacturing in panel construction (Dai et al., 2021), transparent silica glass (Chen et al., 2021), cement mixtures (Ramezanianpour et al., 2021) cement mortar, foundry materials (Kumar Sinha et al., 2021), corrosion protection (Ashrafi-Shahri et al., 2019), automotive engineering (sandblasting) (Cai et al., 2016), etc. Silica sand is one of the most important additive materials and it has been considered by many researchers. It is one of the principal multicomponent materials

due to its stable, environment-friendly, and malleable properties (Ramezanianpour et al., 2021).

The high demand for silica sand products will be directly proportional to the increase in open-pit processing for silica sand purification in the industry (Ben-Awuah et al., 2016). It is noteworthy that open-pit mining also needs to pay attention to land restoration/reclamation after the mining process, to utilize the land for beneficial environmental purposes. The direct impacts of open-pit mining methods are usually complete topsoil removal and altered geomorphological landscapes, which often leave hostile environments to be recolonized by vegetation or animals and directly affect biodiversity and carbon sequestration (Turrión et al., 2021). The illegal mining industry does not carry out post-mining

restoration/reclamation, because it seeks to reduce the production costs (Festin et al., 2019). This condition will impact environmental damage, such as critical land with low nutrients, unstable slope surfaces, low water content, erosion, and sedimentation (García-Ruiz, 2010).

This work specifically studied the characteristics of post-mining soil and solid waste generated from silica sand purification to obtain the reclamation capability of critical land. It is important to identify the characteristics and quality of the soil content, because each region has a different natural state and structure. Natural conditions and weathering processes are some of the reasons why the concentration and structure of silica are different in each country. Open-pit silica mining in the Tuban Regency, Indonesia, has demonstrated a topsoil stripping technique for further exploration of the subgrade containing silica sand. Generally, it has quartz sand and clay, so that silica sand purification is required to obtain α-quartz, β-quartz, α-cristobalite, β-cristobalite, and tridymite (Nurbaiti and Pratapa, 2018; Ratnawulan et al., 2018). Likewise, the solid waste from silica sand purification has wet and sticky characteristics if it contains water, while under dry conditions, it becomes cracked. The samples are clay minerals that contain mineralogical phases, such as anhydrite ($CaSO_4$), quartz (SiO_2), gehlenite ($Ca_2Al(AlSi)O_7$), hematite (Fe_2O_3), and portlandite ($Ca(OH)_2$) that can have interesting characteristics for possible re-use, as a medium for the reclamation of critical land at former silica mines (Perná et al., 2017). Although the reclamation process is difficult to realize using post-mining soil and solid waste, it is necessary to identify initial characteristics to obtain the background data for further research. Several studies have reported on the utilization of post-mining soil and solid waste from the purification of silica sand, such as Hendrychová et al. (2020), who studied the reclamation of ex-mining land in the Czech Republic; Kasztelewicz (2014) examined the land reclamation process after lignite mining in Poland. In addition, Skousen and Zipper (2014) studied post-mining land reclamation in the United States. Many studies on industrial solid waste have also been carried out, including Kawamoto et al. (2021), who examined mine tailings from the Ningyo-toge uranium deposit in Japan. Han et al. (2021) studied the utilization of iron ore tailings being processed into high value-added mesoporous materials. According to Zhang et al.

(2020) and Huang et al. (2020), silica sand tailings can be utilized for ceramic tiles.

This research was conducted as an initial stage on the re-use of solid waste from silica sand purification into post-mining topsoil, especially in the Tuban area, Indonesia. Analysis of the physical, chemical, and biological properties is needed to determine the quality of the soil and make improvements, so that it meets the suitability of the soil, as shown by Lwin et al. (2018). Analysis of the physical characteristics includes aggregate, porosity, and soil texture/structure to determine the ability to drain runoff water to the subsoil. Chemical analysis was performed to observe soil nutrients and heavy metals, whereas biological analysis determined the abundance of bacteria. The results of this early stage of research become the basis for further studies.

MATERIALS AND METHODS

Research location

Post-mining soil sampling was conducted in Latsari Village, Bancar Subdistrict, Tuban Regency, East Java - Indonesia. Specifically, the geographical area is at 6°47'08" South latitude and 111°42'22"East longitude, at an elevation of 56 meters above sea level. In turn, solid waste was obtained from the silica sand purification industry in Jenu Village, Jenu Subdistrict, Tuban Regency, East Java - Indonesia. It is located at 6°50'45.03"South latitude 112°00'41.13"East longitude, with an elevation of 10 meters above sea level.

Sample preparation

Post-mining soil and solid waste sampling were carried out randomly on non-intact, disturbed soil. Samples were taken at 7 locations, at depths of 0, 20, and 50 cm, with as much as 0.5 kg being recovered each time (Susianti et al., 2022; Warmadewanthi et al., 2021a). The samples from different depths were mixed and placed in double plastic, then labeled with the date of collection, place of collection and code. The samples were then tested in the laboratory. For preparation, the samples were sieved on a 100 mm and then used directly in the physical characteristic tests. In the chemical characteristic tests, the samples were dissolved in water containing 10% HNO_3, then distilled for 3 hours to dissolve metal ions.

The samples were filtered to separate solids and solutions. The solutions were tested for AAS and nutrients. For biological characteristics, the sifted samples were dissolved in aquadest and diluted.

Characterization of the materials

Physical characterization

Index soil properties were analyzed, comprising water content (%), coefficient of permeability (cm·s^{-1}), color test, density (g·cm^{-3}), porosity, and particle size distribution (%). The particle size distribution of the two sample types was applied by using the ASTM method, wherein 125 mL of the dispersing agent sodium hexametaphosphate (40 g·L^{-1}) was added to the hydrometer analysis solution (obtained from Merck, Germany) (ASTM E112, 2010). The mixture was stirred until the soil was thoroughly wet and soaked for at least ten minutes. While the soil was soaking, 125 mL of the dispersing agent was added to the control cylinder, which was then filled with distilled water (to the mark). The reading at the top of the meniscus formed by the hydrometer stem and the control solution was taken and (ASTM Alla France series 312H) hydrometer readings were then taken after an elapsed time of 2, 5, 8, 15, 30, and 60 minutes, and 24 hours. In addition, the crystallinity of both samples was also identified using X-ray diffraction (XRD Bruker D8 Advance 3 kW with detector LynxEye XE-T and radiation source Cu K alfa) to identify the crystalline phase in the material. Both samples were analyzed using a Scanning Electron Microscope-E (SEM) Analysis (Hitachi SU-3500 with energy dispersive X-ray (EDX)) operating at a voltage of 5.0 keV and a detector working distance of 11 nm to observe the morphology of the sample regions.

Chemical composition

The chemical analysis of post-mining soil and solid waste was conducted using an inductively coupled, plasma-optical emission spectrometer (ICP-OES type agilent technologies 5100) and atomic absorption spectrophotometer (AAS type Agilent 240FS AA) which aimed to obtain the information regarding the content of heavy metals, such as Barium (Ba), Cadmium (Cd), Lead (Pb), and Zinc (Zn). The chemical compositions were also identified to observe the nutrients in the samples with several tests i.e., water contents (gravimetric), pH (electrometry), C-organic (Walkey &

Black method), total Nitrogen (Kjeldahl), P_2O_5 and K_2O using 25% HCl with a UV-Vis spectrophotometer (Shimadzu – UV-1601 PC). Analysis of the cations exchange was conducted by using the percolation method, coupled with atomic absorption spectrometry (AAS) and titrimetric. Subsequently, these data were compared to Soil Research Center Standards – Agriculture, Indonesia (FLOR, 2005) for a qualified range of good soil properties. Finally, the oxide components in the samples were also identified using X-ray fluorescence (XRF Bruker S2 Puma).

Biological characteristics

The microorganism test was applied using a pour-plate technique with a serial dilution of the mixed culture through a pipette. The molten agar was cooled to 45 °C and poured into a petri dish containing a specified amount of the diluted sample. After the addition of the sample dilution into the molten agar, the plates were gently rotated in a circular motion to achieve uniform distribution of the microorganisms. This procedure was repeated for all sample dilutions to be plated. Dilutions should be plated in duplicate for greater accuracy, incubated overnight, and counted on a colony counter instrument.

RESULTS AND DISCUSSION

Typical samples

Soil has unique characteristics and differs from one area to another, both physically, chemically and biologically. This study observes the characteristics of open-pit silica mining and solid waste refining silica sand in Tuban Regency, East Java Province, Indonesia.

Soil structure is an important aspect of soil quality and ecology and needs to be part of the overall soil quality evaluation framework. According to Mueller et al. (2013), the visual examination and evaluation procedures of soil structure obtain the information on the features and function from macro-morphological characteristics of the soil. Post-mining soil was collected between the clay sand with stone layers at a depth of 30 cm (Figure 1a). Meanwhile, the solid waste was obtained from the resulting clay sand (raw material), purified to obtain the silica sand (Figure 1b). It is clear that the post-mining soil condition has dense contours (clumps), contains rocks and dry

sand, and is light brown in color (Figure 2a-c). In addition, it contains clay minerals with sandy soil contours and forms a soil layer associated with lignite (Figure 2c). The purification system uses a water dispersion system to facilitate high separation (first separator) between stone, organic matter, clay, and silica. This system also obtains clay and silica sand with various particle sizes.

After that, it is re-separated using a water dispersion system to separate the clay and pristine silica, based on particle size > 20 mm. This technique aims to reduce the aluminum and iron content in pristine silica, which can cause clumping of the soil material (Figure 2e). After the separation process, the clay is rejected, and the pristine silica sand is dried at a temperature of 110 °C. Clay is categorized as solid waste from the silica sand purification, because it hardens the material properties when it dries under sunlight. Visually, the solid waste has a light-brown color, contains a lot of water from the water dispersion system, and is dried; it will crack due to lack of water

content (Figure 2d-f). Both samples were tested to assist further study in regenerating critical post-mining land.

Physical properties

In this section, the physical properties were tested to observe the characteristic model of the soil sample. Several tests were carried out, including water content, permeability coefficient, color test, density, porosity, and granularity. In addition, the percentages of sand, clay, and silt were also examined to classify them into triangular textures (Figure 6). On the basis of Table 1, it can be seen that post-mining soil has a low water content compared to solid waste. In silica sand purification, it is clear that the purification process uses a water dispersion system so that the solid waste contains high water content (Figure 4d). This condition is proportional to the coefficient of permeability, where solid waste has small particles that affect the velocity of water
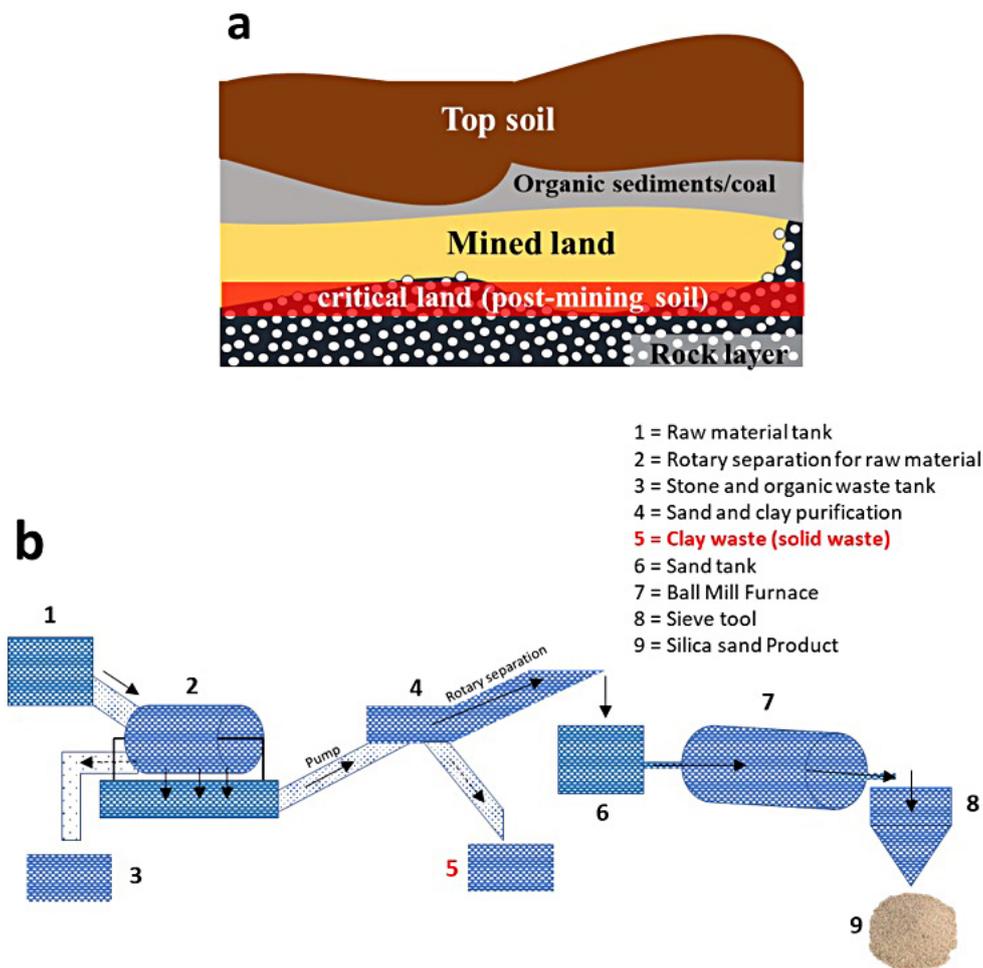
Figure 1. Locations of post-mining soil sampling (a) and solid waste sampling from silica sand purification (b)
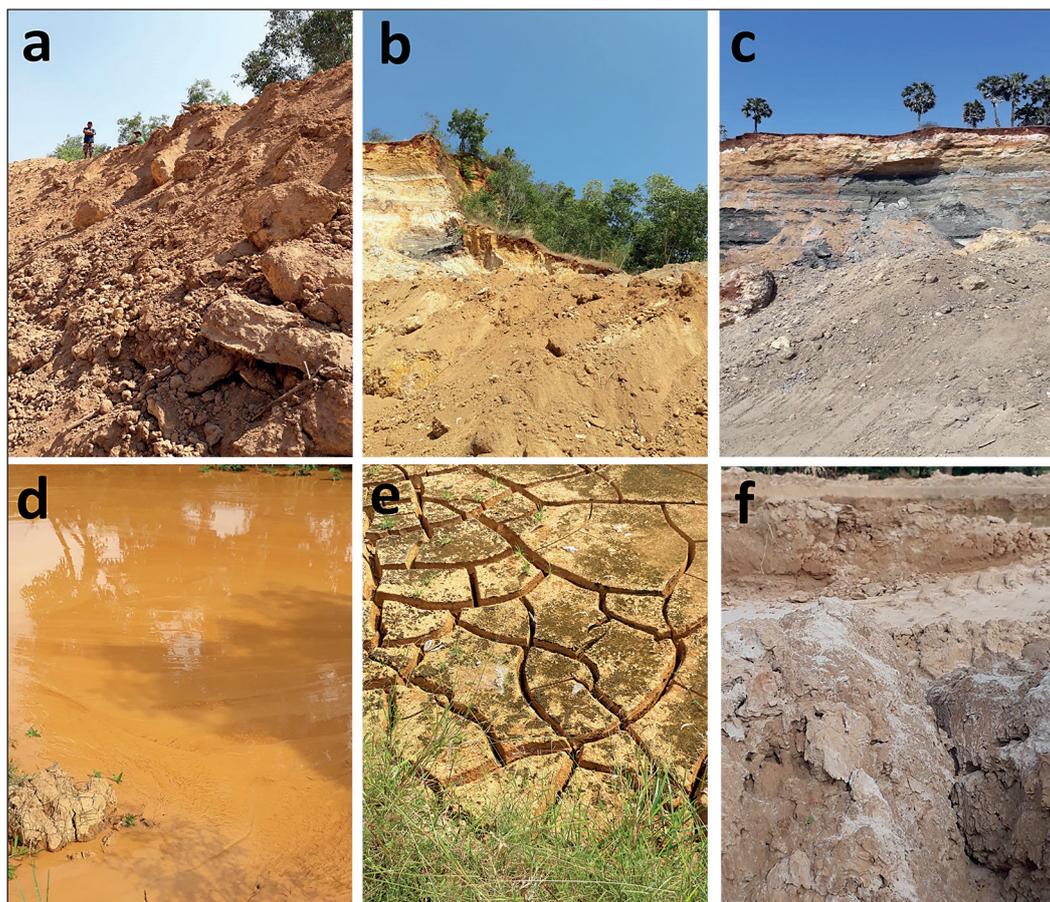
Figure 2. Typical samples: (a, b, c) the post-mining soil and (d, e, f) solid waste from silica sand purification

flow in the soil layer. In addition, a permeability test was carried out to examine the characteristics of post-mining soil and solid waste in its ability to drain runoff water to the subsoil (absorption). Table 2 shows that the permeability data were juxtaposed with the classification of soil permeability by Uhland and Alfred (1951). Table 3 indicates that the sample has been categorized as having very slow permeability. Even though the samples were the same color, they contained clay

minerals, including SiO_2, Al_2O_3, and CaO. Their densities are almost the same, apart from the difference in porosity and gravel content. The small particles of solid waste from silica sand purification will increase the porosity and capability against high-water absorption. Figure 2 shows the particle-size distribution curve, which can be viewed as incremental particle sizes from various post-mining soil; solid waste particle sizes have small increments (on a logarithmic scale) with the

Table 1. The index soil properties of post-mining soil and solid waste

Variable test	Post-mining soil	Solid waste
Water content (%)	3.63	12.57
Coefficient of permeability (cm.s^{-1})	0.69×10^{-6}	1.49×10^{-6}
Color test	Light brown	Light brown
Density (g.cm^{-3})	1.894	1.835
Porosity (%)	35.84	51.12
Gravel (%)	1.51	0.001
Sand (%)	36.95	43.35
Clay (%)	18.80	35.96
Silt (%)	42.74	20.68

Table 2. Permeability classification, according to Uhland and Alfred (1951)

Samples	Permeability (cm/s)	Permeability (cm/h)	Permeability classification (cm/h) [(Uhland and Alfred, 1951)]	Category
Post-mining soil	0.69 × 10⁻⁶	0.2484 × 10⁻²	< 0.0125	Very slow
Solid waste	1.49 × 10⁻⁶	0.5364 × 10⁻²	< 0.0125	Very slow

Table 3. Permeability classification, according to Uhland and Alfred, (1951)

Category	Permeability classification (cm/h)
Very slow	< 0.0125
Slow	0.0125–0.5
Slightly slow	0.5–2.0
Medium	2.0–6.25
Rather fast	6.25–12.5
Fast	12.5–25.5
Very fast	> 25.5

characteristics of multiple mixtures of clay, sand, and silt. The grain-size distribution curve can be divided into small divisions of uniform soil particles and a packing porosity was estimated for the smallest diameter size (Fredlund, 1997). On the basis of the data, the passing percentage of the sand distribution is in the range of 0.850 mm to 0.075 mm. Within a group of soil grains or aggregate, pores of various sizes can be visualized as many interconnecting bottlenecks as possible. The smallest pores at the outermost of an aggregate govern the maximum matric suction of a particular aggregate (or air entry value). Since the pore sizes are not uniform throughout an aggregate, larger pores can be found inside the aggregate. They tend to retain water if surrounded by pores of smaller diameter when the soil is being dried under constant matric suction. Hence, solid waste always has greater water content than post-mining soil (Gallage and Uchimura, 2010). The silica sand can be obtained from open-pit mining in the Tuban regency, with high-silica content of 90 to 98%, after particle separation. As in Table 1, the composition percentage of sand, clay, and silt are plotted into a soil texture triangle so that post-mining soil is classified as clay, while the solid waste from the silica sand purification process is classified as clay and clay loam materials (Figure 3).

On the basis of Figure 4, the two samples have different textures, the post-mining soil including loam and solid waste including clay loam. Loam means that the soil has a composition
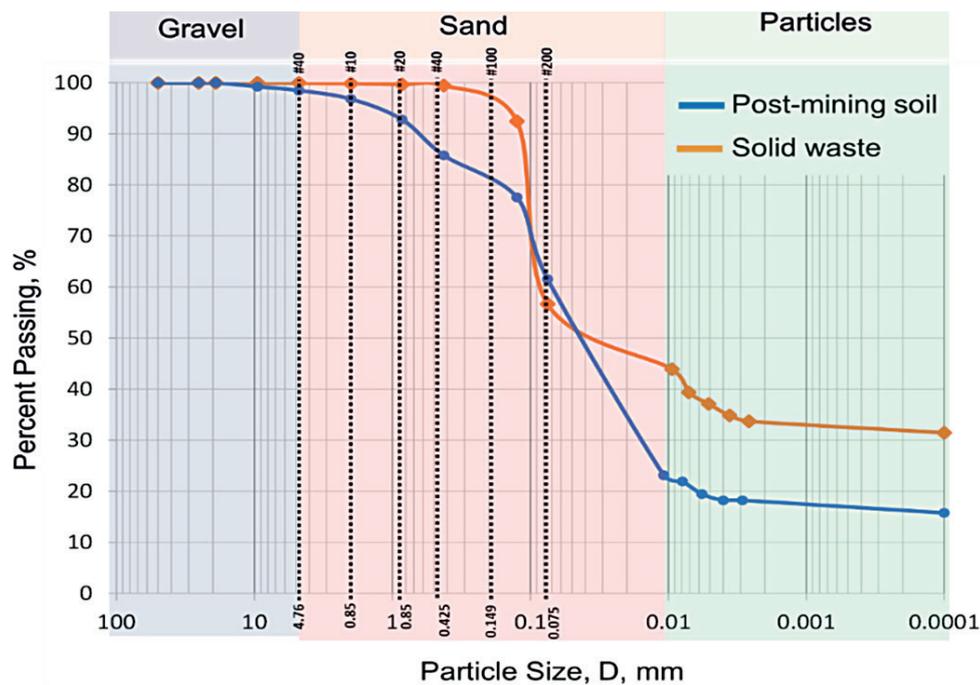
Figure 3. Analysis of post-mining soil and solid waste grain-size distribution curve
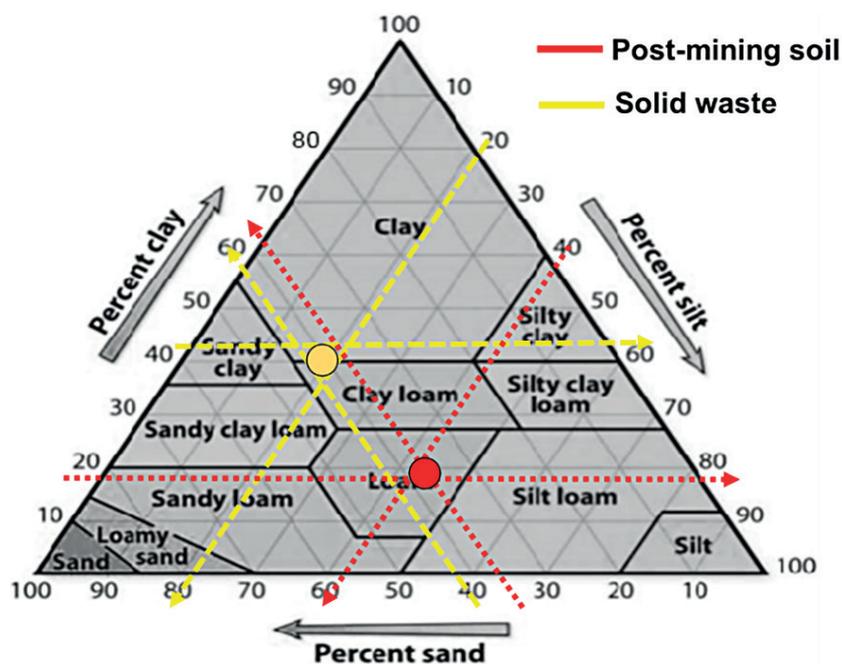
Figure 4. Characteristics of post-mining soil and solid waste in soil texture triangle

of 22.5 to 52.5% sand, 30 to 50% silt, and 10 to 30% clay. Clay loam has a composition of 20 to 45% sand, 15.0 to 52.5% silt and 27.5 to 40% clay (Kaufmann et al., 2011). The XRD pattern in Figure 5 shows that they have the same constituent composition and crystallographic type. In this case, the two patterns are caused by the content of dominant chemicals such as Al_2O_3, MgO, and SiO_2. In addition, the mining land contains some complex chemical mineralogy. This condition is a soil characteristic in the open-pit mining system

in Tuban Regency. On the basis of Figure 5, the XRD pattern of both samples show several clay minerals, such as gehlenite ($Ca_2Al_2SiO_7$), spinel ($MgAl_2O_4$), akermanite ($Ca_2MgSi_2O_7$), monticellite ($CaMgSiO_4$), aluminum oxide (Al_2O_3), magnetite (Fe_3O_4), and hematite (Fe_2O_3). These data have been confirmed by several studies (Dimitrova et al., 2012; Mohassab-Ahmed et al., 2012; Ruíz-Baltazar et al., 2015) which have presented typical XRD patterns of 2 thetas, such as 24.3°, 32.2°, 42.0°, 46.1°, 49.7°, 59.0°, 65.2°, 71.0°,
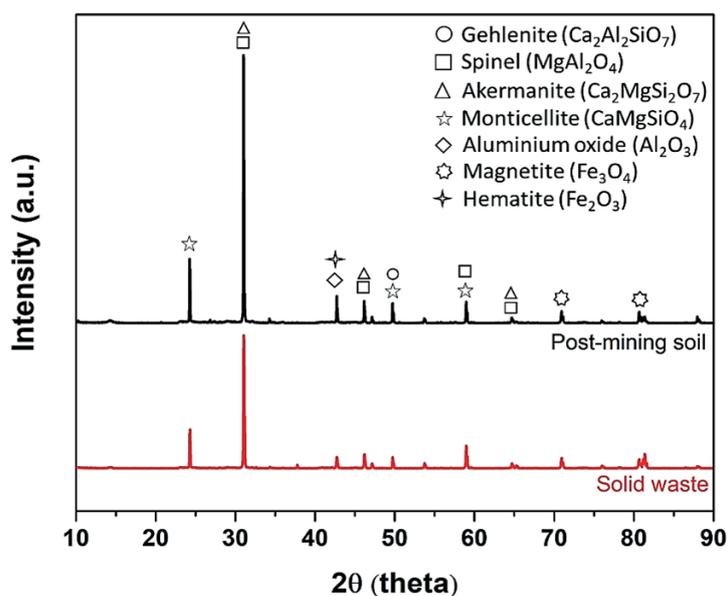
Figure 5. XRD pattern of samples (post-mining soil and solid waste)

80.6°, and 81.0°. The XRD pattern has shown a large number of crystals, formed in both samples, and this is attributed to the magnetite and hematite presenting a cubic structure in which the lattice parameters are very close (Warmadewanthi et al., 2021b). For this reason, it is difficult to differentiate these structures, even if both phases exhibit high crystallinity (Ruíz-Baltazar et al., 2015). This condition also occurs in other minerals caused by the similarity of the constituent elements and crystal lattice. The low intensity was presented by Fe_3O_4 (71.0°, 80.6°, and 81.0°), showing a network of oxygen that presents tetrahedral and octahedral coordination. In turn, the high intensity has been indicated by $CaMgSiO_4$, $Ca_2Al_2SiO_7$, Fe_2O_3, Al_2O_3, $MgAl_2O_4$, and $Ca_2Mg-Si_2O_7$ (at 24.3°, 32.2°, 42.0°, 46.1°, 49.7°, 59.0°, and 65.2°). These minerals have a significant influence on the adsorption properties (clay); most likely, the sample structure and chemical composition characteristics come from the elements Ca, Mg, Si, and Al (Dimitrova et al., 2012).

The particle size, composition, texture, and morphology were also determined using SEM-EDX (Figures 6 and 7). A slight increase in the abundance of particle distribution in solid waste compared to soil-mining soil was observed by low magnification SEM imaging (Figure 6a and 6c); this was consistent with the grain-size distribution (Figure 3) and crystallinity (XRD) analyses. SEM analyses revealed that post-mining soil contained large grains with a composition and morphology consistent with loam. These Si-Fe-C-O-rich grains were observed as akermanite aggregates or particle morphologies similar to those observed by Mihailova et al. (2015) (Figure 7a). The surface was well-crystallized with euhedral crystals which did not exceed 3.0 μm in diameter (Figure 6b). The low silica weight percentage is caused by the ex-mining soil layer reaching the rock layer.

Solid waste has undergone the silica-sand purification system and a concentration process in a water dispersion system, resulting in an increase in the silica content in percentage units of the sample weight. This condition is evidenced by the SEM and EDX results, showing smooth grains with the same composition and morphology as post-mining soil. Low-magnification SEM images (Figure 6b and 6d) suggest that large particles are contained in post-mining soil and smooth particles in solid waste with fractures and porous properties, as reported by Pratiwi et al. (2020). Nevertheless, particles with broadly similar morphologies and textures could be found in both the post-mining and solid waste soil. The composition and texture of both samples were consistent, in terms of some elemental oxides of Ca, Al, Si, and Fe.
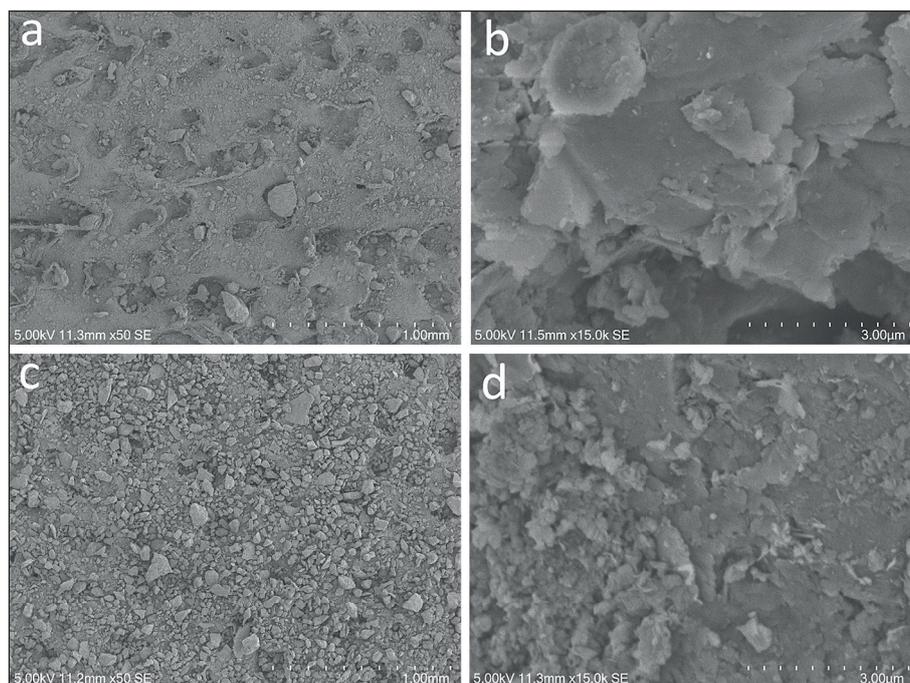
Figure 6. The morphological analysis of both samples with magnification variation; (a, b) post-mining soil, (c, d) solid waste

Post-mining soil		
Elements	Weight %	Atomic %
C	26.4	35.8
O	50.8	51.7
Al	6.3	3.8
Si	12.4	7.2
K	0.7	0.3
Ca	1.2	0.5
Fe	2.1	0.6

Solid waste		
Elements	Weight %	Atomic %
C	19.6	28.1
O	50.1	53.9
Al	4.3	2.8
Si	23.1	14.2
K	0.3	0.1
Ca	0.7	0.3
Fe	1.9	0.6
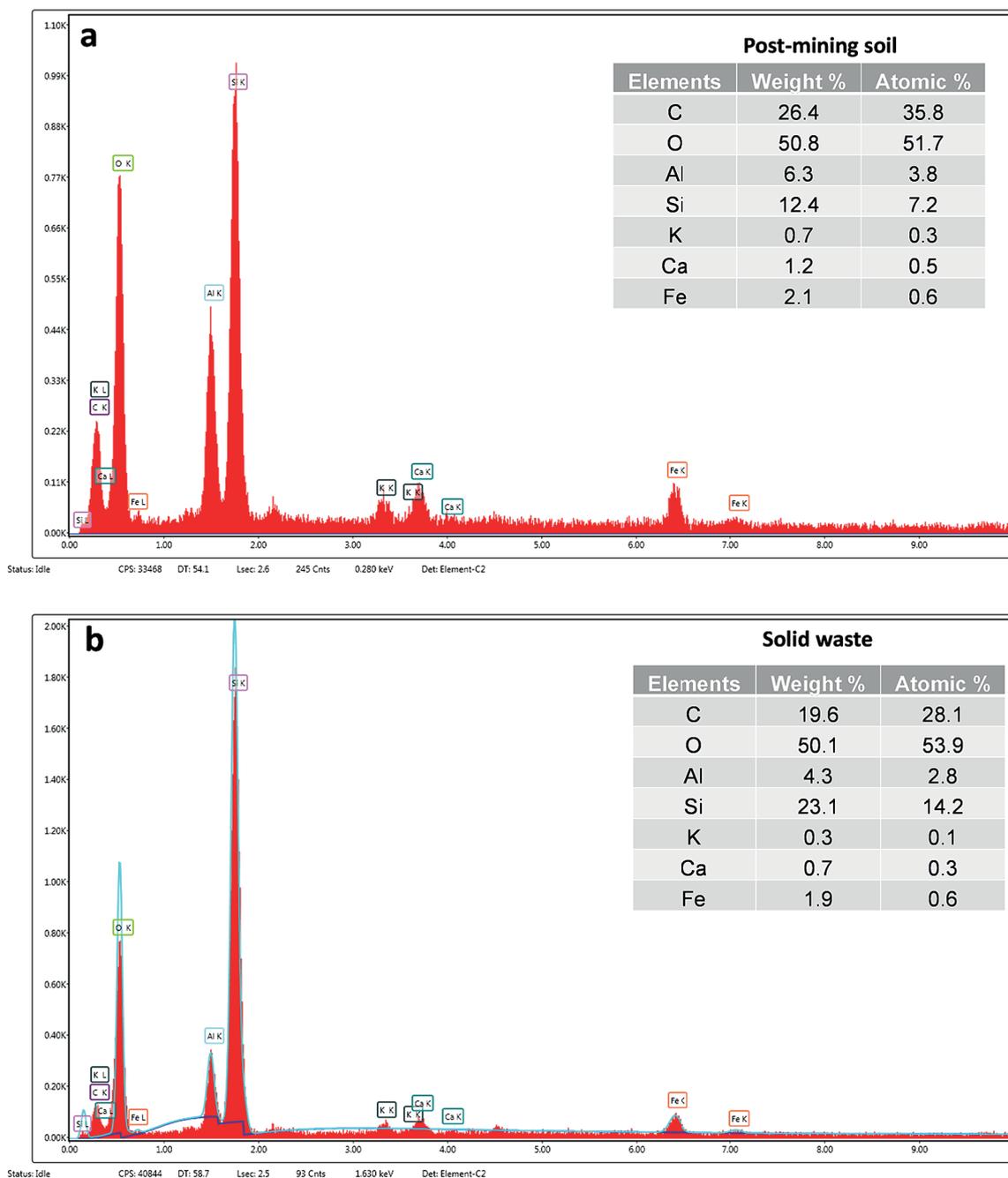
Figure 7. EDX spectrum of both samples; post-mining soil (a) and solid waste (b)

Chemical properties

The chemical properties of samples were also assessed, including the content of heavy metals, soil nutrients, and other oxides using X-Ray Fluorescence (XRF). It is expected that these samples can be applied as modifier materials for the restoration of critical mining lands. On the basis of Table 4, the heavy metal content in solid waste has increased compared to post-mining soil. This is due to the purification of silica sand using a water dispersion process that increases the concentration of heavy metals in solid waste. In addition, it has small particles, thereby increasing particle porosity and promoting high absorption of heavy metals. According to Castro et al. (2020) and Natsir et al. (2021), the clay has pillarization properties when it contains water, meaning that it can increase the formation of lattice spaces that function as metal adsorbents. The data in Table 4 shows that solid waste has greater heavy metal content than post-mining soil.

The soil quality standards on the samples consisting of pH, C-organic, nitrogen, P_2O_5,

Table 4. Chemical content test results from post-mining soil and solid waste

Parameter test	Unit	Post-mining soil	Solid waste	Quality standards (ppm)
Heavy metal contents (Republic of Indonesia government regulations, 2014)				
Barium (Ba)	ppm	87.66 ±2.73	195.06 ±5.46	160
Cadmium (Cd)	ppm	2.40 ±0.06	4.43 ±1.22	3
Chromium (Cr)	ppm	15.34 ±1.15	40.67 ±4.04	76
Lead (Pb)	ppm	4.00 ±3.61	6.00 ±3.61	300
Zinc (Zn)	ppm	19.67 ±0.58	40.67 ±4.93	120
Nutrient contents				
pH H_2O		8.43 ±0.15	8.47 ±0.15	7.45
pH KCl		6.63 ±0.15	7.60 ±0.20	6.60–7.12
C-organic	%	0.23 ±0.05	0.28 ±0.05	2.01–3.00 (medium)
Nitrogen total	%	0.05 ±0.01	0.05 ±0.01	0.21–0.50 (medium)
P_2O_5 potential	mg/100 g	11.30 ±0.57	17.67 ±6.65	21.00–40.00 (medium)
K_2O potential	mg/100 g	7.67 ±0.57	42.33 ±19.01	21.00–40.00 (medium)
Cations exchanged				
K	cmoll(+) kg^{-1}	0.16 ±0.05	0.19 ±0.05	0.30–0.50 (medium)
Ca	cmoll(+) kg^{-1}	5.21 ±1.21	6.70 ±1.60	11.00–20.00 (medium)
Mg	cmoll(+) kg^{-1}	1.38 ±0.34	2.00 ±0.39	2.10–8.00 (medium)
Na	cmoll(+) kg^{-1}	0.11 ±0.02	0.21 ±0.07	0.80–1.00 (medium)
Cation exchange capacity		4.07 ±0.30	10.01 ±4.09	17.00–24.00 (medium)

and K_2O content and ion exchange capacity were also reported to determine nutrient composition. Solid waste gave a high-value increase compared to post-mining soil. This data compares with the standards of the Agricultural Research and Development Agency, Ministry of Agriculture Indonesia (2005), and indicates that the soil quality standards in the sample are in a reasonably good range below the standard soil content. More specifically, the chemical compositions derived from XRF instruments were presented and it is clear that both samples have different characteristics. Table 5 shows that post-mining soil has a high chemical composition of 100%, which indicates a high chemical content of SiO_2, Al_2O_3, CaO, and MgO. The loss of ignition (LoI) represents the material lost during smelting or refining in a furnace or smelter, such as loss of organic constituents and water content. The low LoI data characterizes that the sample is dry and usually contains a lot of rock. In addition, post-mining soil was collected from incomplete soil composites with a thickness of 0-20 cm of soil extraction from ex-mining land (Figure 1a). Meanwhile, solid waste from silica sand purification is presented with low chemical content, characterized by clay, which contains SiO_2 and Al_2O_3.

Biological properties

Bacterial growth testing was evaluated to determine the level of fertility of the sample. One of the parameters of soil fertility is the level of organism, which helps increase the decomposition of organic matter. According to Tangahu (2017), the best number of colonies that can be counted ranges from 30 to 300 microbes per mL or per gram sample. This study identified two dilution variables (10-4 and 10-5) to find the lowest point for viable bacteria. On the basis of Table 1, it can be seen that there is a relationship between nutrients and soil permeability. Solid waste has sand aggregate, which contains more nutrients and is better than post-mining soil. In addition, the high-water content will be proportional to the increase in bacterial growth and the high abundance of microorganisms will change the soil structure from single grains to lumps. Table 6 on the 10^{-5} dilution of post-mining soil did not identify bacterial growth, while the solid waste contained 1.64×10^5 bacteria.

CONCLUSIONS

On the basis of the analysis of the physical characteristics test that has been applied, concerning ASTM 112-10, it was shown that

Table 5. The chemical composition of post-mining soil and solid waste from silica sand purification

Elements	Post-mining soil (% wt)	Solid waste (% wt)
SiO_2	66.86	64.58
Fe_2O_3	3.40	3.60
Al_2O_3	21.70	17.18
CaO	3.20	2.75
MgO	1.30	0.77
TiO_2	0.90	0.80
K_2O	1.50	1.69
Na_2O	0.01	0.10
MnO_2	0.01	0.03
Cr_2O_3	0.01	0.01
LoI	1.11	7.93
Total	100.00	99.44

Table 6. The abundance of post-mining soil and solid waste organisms (CFU)

Process	Post-mining soil (a)	Solid waste (b)
Dilution 10^{-4}	1.59×10^3	4.10×10^5
Dilution 10^{-5}	0	1.64×10^5

the post-mining soil contains 36.95% sand, 18.80% clay, and 42.74% silt, with a permeability and porosity coefficient of 0.69×10^{-6} cm·s^{-1} and 35.84%. Meanwhile, the solid waste contains 43.35% sand, 35.96% clay, and 20.68% silt with a permeability and porosity coefficient of 1.49×10^{-6} cm·s^{-1} and 51.12%. Overall, the mineralogy and morphology of the two samples showed the same chemical composition as gehlenite ($Ca_2Al_2SiO_7$), spinel ($MgAl_2O_4$), akermanite ($Ca_2MgSi_2O_7$), monticellite ($CaMgSiO_4$), aluminium oxide (Al_2O_3), magnetite (Fe_3O_4), and hematite (Fe_2O_3) with euhedral crystals not exceeding 3.0 m in diameter. The XRF instrument supports the analysis from the chemical characteristics test that the chemical composition of the two samples is SiO_2, Al_2O_3, CaO, and MgO, but the post-mining soil has a low content of heavy metals and nutrients compared to solid waste. Meanwhile, solid waste has a high heavy metal and nutrient content, due to leaching and binding from the silica sand refining process. The analysis of biological characteristics showed that the abundance of bacteria (CFU) for the 4th and 5th dilutions in post-mining soil was 1.59×10^3 and was not detected, whereas in solid waste, it was 4.10×10^5 and 1.64×10^5. From the above test results, solid waste can be recovered into topsoil material by carrying out two steps, namely immobilizing heavy metals, cadmium and barium. Furthermore, nutrients need to be added in order to meet the quality standards. The resulting topsoil material will later be used to reclaim mining land.

Acknowledgments

REFERENCES

1. Ashrafi-Shahri, S.M., Ravari, F., Seifzadeh, D. 2019. Smart organic/inorganic sol-gel nanocomposite containing functionalized mesoporous silica for corrosion protection. Prog. Org. Coatings, 133, 44–54.

2. ASTM E112. 2010. Standard Test Methods for Determining Average Grain Size E112-10. Astm E112-10 96, 1–27. https://doi.org/10.1520/E0112-10.

3. Ben-Awuah, E., Richter, O., Elkington, T., Pourrahimian, Y. 2016. Strategic mining options optimization: Open pit mining, underground mining or both. Int. J. Min. Sci. Technol., 26, 1065–1071.

4. Cai, X., He, Z., Tang, S., Chen, X. 2016. Abrasion erosion characteristics of concrete made with moderate heat Portland cement, fly ash and

silica fume using sandblasting test. Constr. Build. Mater., 127, 804–814. https://doi.org/10.1016/j.conbuildmat.2016.09.117

5. Castro, A., Amaya, J., Molina, R., Moreno, S. 2020. Pillarization in concentrated media with solid Al and Al-Zr polymers to obtain acid catalysts. Catal. Today, 356, 284–291.

6. Chen, Y.H., Hu, X., Lin, T., Li, Y., Ling, Z.Y. 2021. Obtaining transparent silica glass from nano-silica hydrosol. Ceram. Int., 47, 19340–19345. https://doi.org/10.1016/j.ceramint.2021.03.270

7. Dai, X., Liu, H., Liu, X., Liu, Z., Liu, Y., Cao, Y., Tao, J., Shan, Z. 2021. Silicon nanoparticles encapsulated in multifunctional crosslinked nano-silica/carbon hybrid matrix as a high-performance anode for Li-ion batteries. Chem. Eng. J., 418, 129468. https://doi.org/10.1016/j.cej.2021.129468

8. Dimitrova, S.V., Mihailova, I.K., Nikolov, V.S., Mehandjiev, D.R. 2012. Adsorption capacity of modified metallurgical slag. Bulg. Chem. Commun., 44, 30–36.

9. Festin, E.S., Tigabu, M., Chileshe, M.N., Syampungani, S., Odén, P.C. 2019. Progresses in restoration of post-mining landscape in Africa. J. For. Res., 30, 381–396.

10. FLOR, A.G. 2005. Ministry of agriculture indonesian agency for agricultural research and development.

11. Fredlund, M.D., 1997. Prediction of the soil-water characteristic curve from grain-size distribution and volume-mass properties. Can. Geotech. J., 39, 1103.

12. Gallage, C.P.K., Uchimura, T. 2010. Effects of dry density and grain size distribution on soil-water characteristic curves of sandy soils. Soils Found, 50, 161–172. https://doi.org/10.3208/sandf.50.161

13. García-Ruiz, J.M. 2010. The effects of land uses on soil erosion in Spain: A review. Catena, 81, 1–11. https://doi.org/10.1016/j.catena.2010.01.001

14. Han, X., Wang, Y., Zhang, N., Meng, J., Li, Y., Liang, J. 2021. Facile synthesis of mesoporous silica derived from iron ore tailings for efficient adsorption of methylene blue. Colloids Surfaces A Physicochem. Eng. Asp., 617, 126391.

15. Hendrychová, M., Svobodova, K., Kabrna, M. 2020. Mine reclamation planning and management: Integrating natural habitats into post-mining land use. Resour. Policy, 69, 101882.

16. Huang, Q., Liu, T., Zhang, J., He, X., Liu, J., Luo, Z., Lu, A. 2020. Properties and pore-forming mechanism of silica sand tailing-steel slag-coal gangue based permeable ceramics. Constr. Build. Mater., 253, 118870.

17. Kasztelewicz, Z. 2014. Approaches to post-mining land reclamation in Polish open-cast lignite mining. Civ. Environ. Eng. Reports.

18. Kaufmann, R.K., Kauppi, H., Mann, M.L., Stock, J.H. 2011. Reconciling anthropogenic climate change with observed temperature 1998–2008, Proceedings of the National Academy of Sciences. National Acad Sciences.

19. Kawamoto, K., Yokoo, H., Ochiai, A., Nakano, Y., Takeda, A., Oki, T., Takehara, M., Uehara, M., Fukuyama, K., Ohara, Y. 2021. The role of nanoscale aggregation of ferrihydrite and amorphous silica in the natural attenuation of contaminant metals at mill tailings sites. Geochim. Cosmochim. Acta, 298, 207–226.

20. Kumar Sinha, N., Kumar, J., Choudhary, I.N., Prasad, R., Singh, J.K. 2021. Utilization of industrial solid waste as a mold material in the foundry industry. Mater. Today Proc., 46, 1492–1498. https://doi.org/10.1016/j.matpr.2020.11.748

21. Mihailova, I., Radev, L., Aleksandrova, V., Colova, I., Salvado, I., Fernandes, M. 2015. Novel merwinite/akermanite ceramics: in vitro bioactivity. Bulg Chem Commun, 47, 253–260.

22. Mohassab-Ahmed, M.Y., Sohn, H.Y., Kim, H.G. 2012. Sulfur distribution between liquid iron and magnesia-saturated slag in H2/H2O atmosphere relevant to a novel green ironmaking technology. Ind. Eng. Chem. Res., 51, 3639–3645.

23. Mueller, L., Shepherd, G., Schindler, U., Ball, B.C., Munkholm, L.J., Hennings, V., Smolentseva, E., Rukhovic, O., Lukin, S., Hu, C. 2013. Evaluation of soil structure in the framework of an overall soil quality rating. Soil Tillage Res., 127, 74–84.

24. Natsir, M., Putri, Y.I., Wibowo, D., Maulidiyah, M., Salim, L.O.A., Azis, T., Bijang, C.M., Mustapa, F., Irwan, I., Arham, Z. 2021. Effects of Ni–TiO2 pillared Clay–Montmorillonite composites for photocatalytic enhancement against reactive orange under visible light. J. Inorg. Organomet. Polym. Mater., 31, 3378–3388.

25. Nurbaiti, U., Pratapa, S. 2018. Synthesis of cristobalite from silica sands of Tuban and Tanah Laut. J. Phys. Conf. Ser., 983. https://doi.org/10.1088/1742-6596/983/1/012014

26. Perná, I., Šupová, M., Hanzlíček, T. 2017. The characterization of the Ca-K geopolymer/solidified fluid fly-ash interlayer. Ceram. - Silikaty, 61, 26–33. https://doi.org/10.13168/cs.2016.0056

27. Pratiwi, W., Karim, G.A., Rachmawati, T. 2020. Local silica sand as a substitute for standard ottawa sand in testing of cement mortar, in: Materials Science Forum. Trans Tech Publ, 220–226.

28. Ramezanianpour, A.A., Mortezaei, M., Mirvalad, S. 2021. Synergic effect of nano-silica and natural pozzolans on transport and mechanical properties of blended cement mortars. J. Build. Eng., 44. https://doi.org/10.1016/j.jobe.2021.102667

29. Ratnawulan, R., Fauzi, A., Hayati, A.E.S. 2018. Characterization of Silica Sand Due to the Influence of Calcination Temperature. IOP Conf. Ser. Mater. Sci. Eng., 335, 0–5. https://doi.

org/10.1088/1757-899X/335/1/012008

30. Ruíz-Baltazar, A., Esparza, R., Rosas, G., Pérez, R. 2015. Effect of the surfactant on the growth and oxidation of iron nanoparticles. J. Nanomater., 2015.

31. Santos, M.F.M., Fujiwara, E., Schenkel, E.A., Enzweiler, J., Suzuki, C.K. 2015. Processing of quartz lumps rejected by silicon industry to obtain a raw material for silica glass. Int. J. Miner. Process., 135, 65–70. https://doi.org/10.1016/j.minpro.2015.02.002

32. Skousen, J., Zipper, C.E. 2014. Post-mining policies and practices in the Eastern USA coal region. Int. J. coal Sci. Technol., 1, 135–151.

33. Susianti, B., Warmadewanthi, I.D.A.A., Tangahu, B.V. 2022. Characterization and experimental evaluation of cow dung biochar + dolomite for heavy metal immobilization in solid waste from silica sand purification. Bioresour. Technol. Reports 18, 101102. https://doi.org/10.1016/j.biteb.2022.101102

34. Tangahu, B.V. 2017. Bioremediation of Oil Contaminated Soil by Biostimulation Method Using NPK Fertilizer. Open Access Libr. J., 4, 1.

35. Turrión, D., Morcillo, L., Alloza, J.A., Vilagrosa, A. 2021. Innovative techniques for landscape recovery after clay mining under mediterranean conditions. Sustain., 13, 1–18. https://doi.org/10.3390/su13063439

36. Uhland, R.E., Alfred, M. 1951. Soil permeability determinations for use in soil and water conservation. LWW.

37. Warmadewanthi, I.D.A.A., Chrystiadini, G., Kurniawan, S.B., Abdullah, S.R.S. 2021a. Impact of degraded solid waste utilization as a daily cover for landfill on the formation of methane and leachate. Bioresour. Technol. Reports, 15. https://doi.org/10.1016/j.biteb.2021.100797

38. Warmadewanthi, I.D.A.A., Zulkarnain, M.A., Ikhlas, N., Kurniawan, S.B., Abdullah, S.R.S. 2021b. Struvite precipitation as pretreatment method of mature landfill leachate. Bioresour. Technol. Reports, 15, 100792. https://doi.org/10.1016/j.biteb.2021.100792

39. Zhang, J., Liu, T., Huang, Q., Luo, Z., Lu, A., Zhu, L. 2020. Preparation, properties characterization and structure formation mechanism of silica sand tailings-based ceramic materials. Mater. Chem. Phys., 255, 123611.